NEW MEXICO INSTITUTE OF MINING AND TECHNOLOGY

A THEORETICAL STUDY OF INDUCED ELECTRICAL POLARIZATION

BY

RICHARD H. FRISCHE

Submitted in Partial Fulfillment of the
Requirements for the Degree of
Master of Science in Earth Science at the
New Mexico Institute of Mining and Technology

SOCORRO, NEW MEXICO
June, 1956

ACKNOWLEDGEMENT

The writer wishes to express his appreciation to Dr. Haro von Buttlar who served as advisor for this problem. Also deserving of special thanks are Professor Victor Vacquier, Dr. C.R. Cassity, and Mr. Charles R. Holmes of the New Mexico Institute of Mining and Technology faculty whose guidance was extremely helpful in developing this paper. Dr. Nicholas Metropolis and Miss Sandra Swan of Los Alamos Scientific Laboratory donated their aid in the setting up and in the machine computation of the integral derived in this study. For the drafting and typing of this paper I am indebted to Maureen Frische.

ABSTRACT

A mathematical solution was obtained and numerically evaluated for determining the depth to a saturated aquifer when prospecting for ground water by induced electrical polarization. In a horizontally stratified earth model consisting of a nonpolarizable overburden and of an underlying infinitely deep polarizable layer, the induced-polarization potential difference for a Wenner electrode configuration is fairly independent of the resistivity contrast. The computation agrees with results from a laboratory model tank and with a field curve. This increases confidence in the validity of the results obtained from the model tank on earth models too complex for computation.

TABLE OF CONTENTS

LIST OF FIGURES

LIST OF TABLES

INTRODUCTION

When an aquifer contaminated with clay minerals and saturated with water is made to conduct direct current, it becomes electrically polarized as though it consisted of a mass of little condensers filled with a leaky dielectric. Dry earth materials do not exhibit this effect. At New Mexico Institute of Mining and Technology, field experiments have been underway for 2½ years to determine whether this electrical polarization of clay-contaminated aquifers can be used for locating new supplies of ground water. In this paper a mathematical expression for the polarization effect is derived and numerically evaluated for a simple earth model in order to guide experimental model studies in the laboratory and help to interpret field measurements.

The field procedure consists of sending a direct current I (measured at A) through electrodes 1) and 2), as shown in Figure 1, for a given length of time, interrupting this current, and recording a few milliseconds later the voltage between electrodes 3) and 4). Usually the ground is energized for 30 seconds and the decay of the relaxation voltage is observed for two minutes. The value of the relaxation voltage immediately after the current is shut off is designated by $\Delta\phi$. In the field $\Delta\phi$ is of the order of 10 millivolts, whereas when the current is flowing the voltage V between electrodes 3) and 4) is of the order of one volt. Paul Kintzinger (1956) has demonstrated that the ratio $\frac{\Delta\phi}{V}$ is

WENNER CONFIGURATION

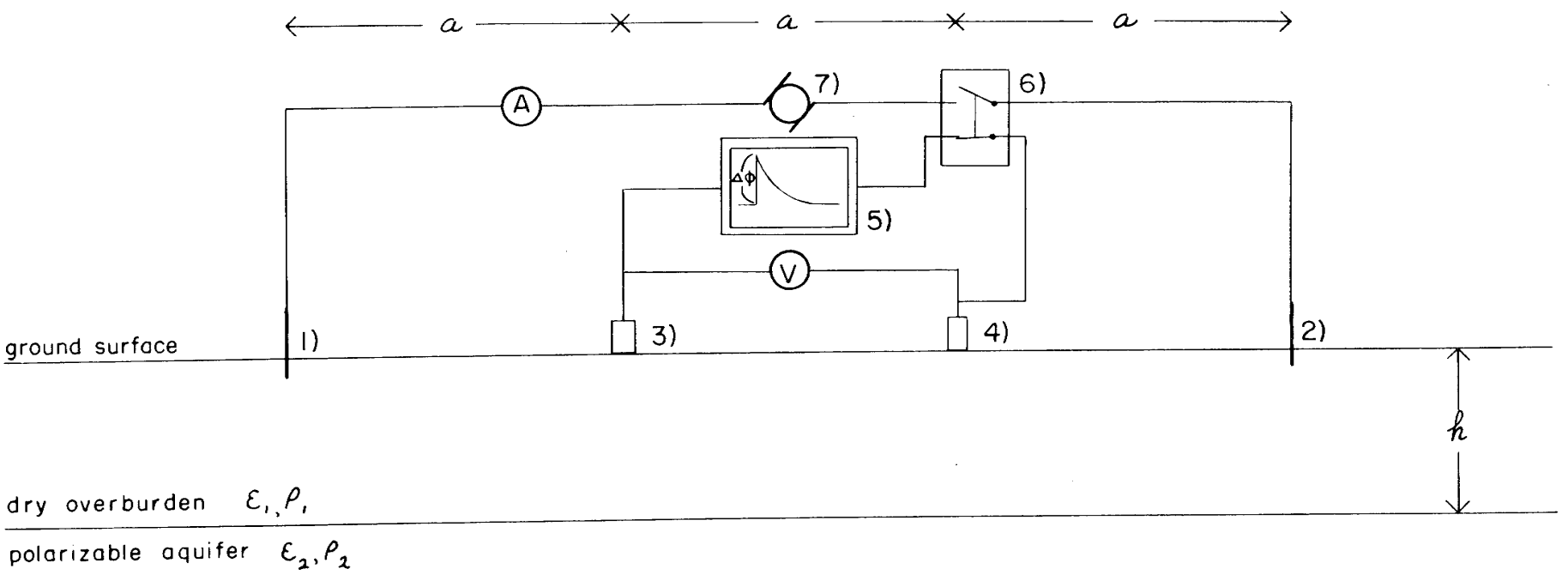

1) and 2) are current electrodes
3) and 4) are nonpolarizing electrodes
5) is a decay voltage amplifier and recorder
6) is a microswitch
7) is a D.C. generator

(A) is a D.C. ammeter
(V) is a voltmeter
ρ is the resistivity
ε is the electric permittivity

Figure 1

independent of the value of V, and therefore this ratio represents a specific property of the aquifer, namely its polarizability. Since $\Delta\phi$ is two orders of magnitude smaller than V its detection is difficult by alternating-current methods. Because the relaxation voltage is long, taking 15 seconds to drop to half value, $\Delta\phi$ is easily observed after the current is shut off. The time dependence of this decay is the same for all portions of the uniform aquifer. The present study does not consider the physico-chemical mechanism by which the ground acquires polarization or the various factors which influence its decay. The study is entirely restricted to the determination of $\frac{\Delta\phi}{V}$ as a function of the Wenner electrode spacing a for the case of a horizontally stratified-earth model. The values of $\frac{\Delta\phi}{V}$ for two values of the electrode spacing a will bear the same ratio to each other for any chosen time interval measured from the instant the energizing current is broken. This ratio is also independent of the length of time the ground is energized. Thus time does not enter into the equations.

The earth model that was used is shown in Figure 1. It consists of a dry overburden of uniform thickness h, possessing an electric permittivity ε_1, and a resistivity ρ_1; and of a saturated aquifer of electric permittivity ε_2 and resistivity ρ_2 extending to infinity below this depth h. Curves were computed for $\Delta\phi$ as a function of the electrode spacing a for various ratios of ρ_1 to ρ_2. It was assumed that only the lower layer was polarizable, the permittivity of the air and of the upper

layer always being that of vacuum. The electrical behavior of the aquifer is assumed to be completely defined by its resistivity and dielectric constant, even though the aquifer certainly is not a dielectric in the conventional sense.

Since Kintzinger has shown that $\frac{\Delta\Phi}{V}$ is independent of the value of the exciting current, it follows that the polarization of each volume element of the aquifer can be expressed as a constant times the current density vector. The polarization can be expressed as

$$\vec{P} = \varepsilon_o \chi_e \vec{E}$$

where ε_o is the permittivity of a vacuum and χ_e is the susceptibility of the polarizable medium. The current density is

$$\vec{J} = \frac{\vec{E}}{\rho} \quad .$$

The potential function in each medium can therefore be calculated from the current flow. It is shown that polarization does not enter into this calculation and that the expressions developed by Roman (1931) for the potential in the case of current flow in a two-layered earth model are valid. This implies that the ground has been energized long enough so that the current has reached a steady-state value. Under these conditions it is customary to treat the current-flow problem by the electrostatic analogy in which charges of $\frac{I\rho_1}{2\pi}$ replace the current electrodes.

After the current is shut off, the polarization of the aquifer is the only source of potential difference at the potential electrodes. Therefore the derivation is concerned with the calculation

of the potential difference at the potential electrodes due to a polarized volume element of the aquifer. The potential $d\phi$ at a distance r from the polarized volume element $d\tau$ is

$$d\phi = \frac{|\vec{P}| \cos\theta}{4\pi\varepsilon r^2} d\tau$$

where θ is the angle between the direction of the dipole moment vector and the vector $\vec{r}$. The difference of potential measured at the location of the potential electrodes due to the polarized volume element is then (Figure 2)

$$d\phi_3 - d\phi_4 = \frac{|\vec{P}|}{4\pi\varepsilon} \left(\frac{\cos\theta_3}{r_3^2} - \frac{\cos\theta_4}{r_4^2} \right) d\tau \quad .$$

POLARIZATION COMPONENTS OF
POLARIZED VOLUME ELEMENT

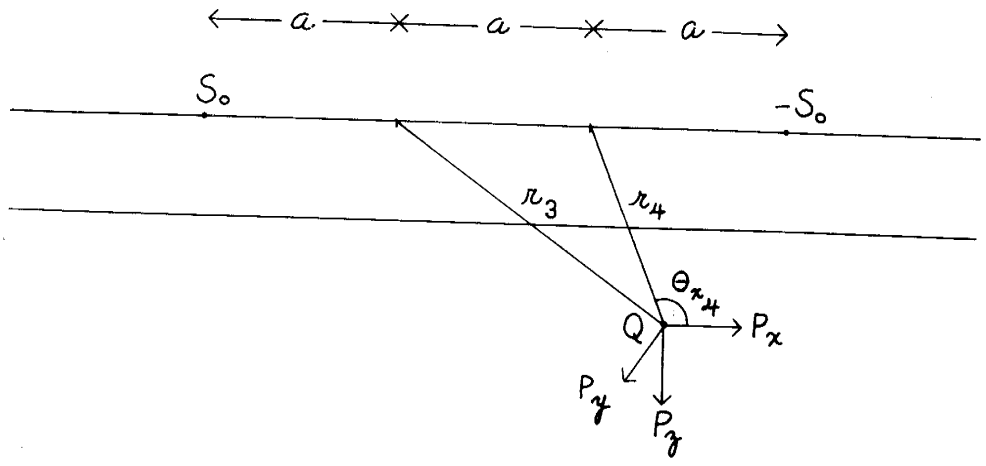

Figure 2

Next, the expression has to be integrated over the total volume of the aquifer to yield the measured $\Delta\phi$,

$$\Delta\phi = \int_{\text{aquifer}} \frac{|\vec{P}|}{4\pi\varepsilon}\left(\frac{\cos\theta_3}{r_3^2} - \frac{\cos\theta_4}{r_4^2}\right) d\tau \quad .$$

Finally, in order to get an expression for $\frac{\Delta\phi}{V}$, the quantity V has to be related to the electrical constants of the ground. Wenner's formula for the potential difference between electrodes 3) and 4) (Figure 1) is

$$V = \frac{I\rho_a}{2\pi a}$$

where ρ_a is the apparent resistivity of the ground at a particular electrode separation a.

The expression $\frac{\Delta\phi}{V}$ thus obtained will then be compared to field observations.

THEORETICAL DEVELOPMENT

Proof That the Current Distribution Is Independent of the Polarization

Maxwell's equations lead to the following boundary conditions for the two-layer case:

1) the potential is steady across the interfaces, i.e.

$$\Psi_0 = \Psi_1$$

at $z = 0$, and (1)

$$\Psi_1 = \Psi_2$$

at $z = h$;

2) the normal component of the current density vector $J_z = -\frac{1}{\rho}\frac{\partial \Psi}{\partial z}$ is steady, i.e.

$$\frac{1}{\rho_0}\frac{\partial \Psi_0}{\partial z} - \frac{1}{\rho_1}\frac{\partial \Psi_1}{\partial z} = 0$$

at $z = 0$, and (2)

$$\frac{1}{\rho_1}\frac{\partial \Psi_1}{\partial z} - \frac{1}{\rho_2}\frac{\partial \Psi_2}{\partial z} = 0$$

at $z = h$;

3) the normal component of the electric displacement vector $D_z = -\varepsilon\frac{\partial \Psi}{\partial z}$ changes by an amount equal to the free surface

charge density ω_f on the interface, i.e.

$$\varepsilon_0 \frac{\partial \psi_0}{\partial z} - \varepsilon_1 \frac{\partial \psi_1}{\partial z} = \omega_f'$$

at $z = 0$, and (3)

$$\varepsilon_1 \frac{\partial \psi_1}{\partial z} - \varepsilon_2 \frac{\partial \psi_2}{\partial z} = \omega_f$$

at $z = h$.

ψ_0 , ψ_1 and ψ_2 are the potentials in the 0), 1), and 2) media respectively (Figure 3). From these equations it is apparent that if neither the overburden nor the aquifer is polarizable, a free surface charge density of

$$\omega_f = \varepsilon_0 \left(\frac{\partial \psi_1}{\partial z} - \frac{\partial \psi_2}{\partial z} \right) \tag{4}$$

will reside on the $z = h$ interface. Since no bound charges occur in this case, ω_f represents the total charge density on the interface.

SURFACE CHARGE DISTRIBUTION ON $z = h$ INTERFACE

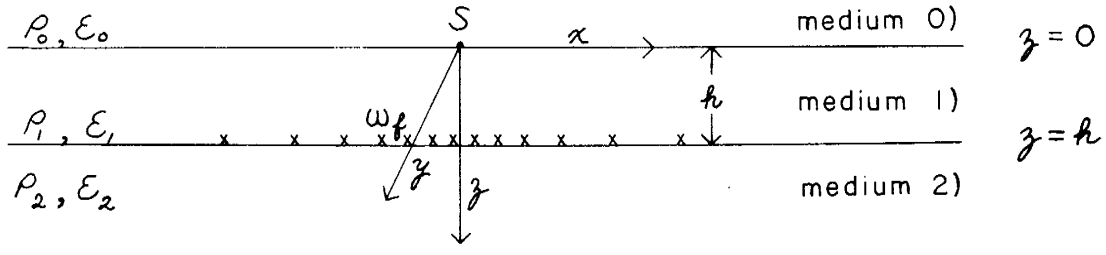

Figure 3

In the induced polarization case where the lower medium is polarizable there will be an additional contribution to the surface charge on the interface due to the volume polarization. A question arises as to whether this changes the current distribution between media 1) and 2). In the general case where the media are polarizable and conducting, the surface-charge density on the interface will be comprised of free charge due to the conductivity difference between the two media, and bound charge due to the difference in dielectric constants.

The bound surface charge density can be developed from the relation

$$div\,\vec{P} = -\delta' \tag{5}$$

where δ' is the bound volume charge density. This relation gives rise to

$$P_{z_1} - P_{z_2} = \omega_b \tag{6}$$

where ω_b is the bound surface charge on the interface. Since

$$\vec{P} = \varepsilon_o \chi_e \vec{E} \tag{7}$$

and

$$\vec{E} = -\nabla\psi \quad , \tag{8}$$

$$P_z = -\varepsilon_o \chi_e \frac{\partial \psi}{\partial z} \quad . \tag{9}$$

The relation between susceptibility and permittivity is.

$$\chi_e = \frac{\varepsilon}{\varepsilon_o} - 1 \tag{10}$$

or

$$\varepsilon_o \chi_e = \varepsilon - \varepsilon_o \quad . \tag{10'}$$

Thus the above boundary condition may be rewritten as

$$-\varepsilon_1 \frac{\partial \psi_1}{\partial z} + \varepsilon_o \frac{\partial \psi_1}{\partial z} + \varepsilon_2 \frac{\partial \psi_2}{\partial z} - \varepsilon_o \frac{\partial \psi_2}{\partial z} = \omega_b \quad . \tag{11}$$

The total surface charge ω is the sum of ω_f and ω_b:

$$\omega = \varepsilon_o \frac{\partial \psi_1}{\partial z} - \varepsilon_o \frac{\partial \psi_2}{\partial z} \quad . \tag{12}$$

Equation (12) is obviously the expression for the surface charge density in the case of nonpolarizable media (equation 4).

This shows that the current distribution is not affected by the dielectric polarization. Therefore the method used by Roman (1931) for determining the potentials in a horizontally-stratified earth model is valid for the polarization problem.

Computation of the Induced-Polarization Quantity $\frac{\Delta \phi}{V}$

Probably the simplest way of determining the potentials in the different media for the two-layer case is the image method (Roman, 1931). In Figure 4, the point S_o, taken as the origin, is a constant point charge representing the current electrode after the establishment of the steady-state condition. M_2 is its image across the interface between medium 1) and medium 2). N_2 is the image of M_2 across the interface between medium 0)

IMAGES OF SOURCE

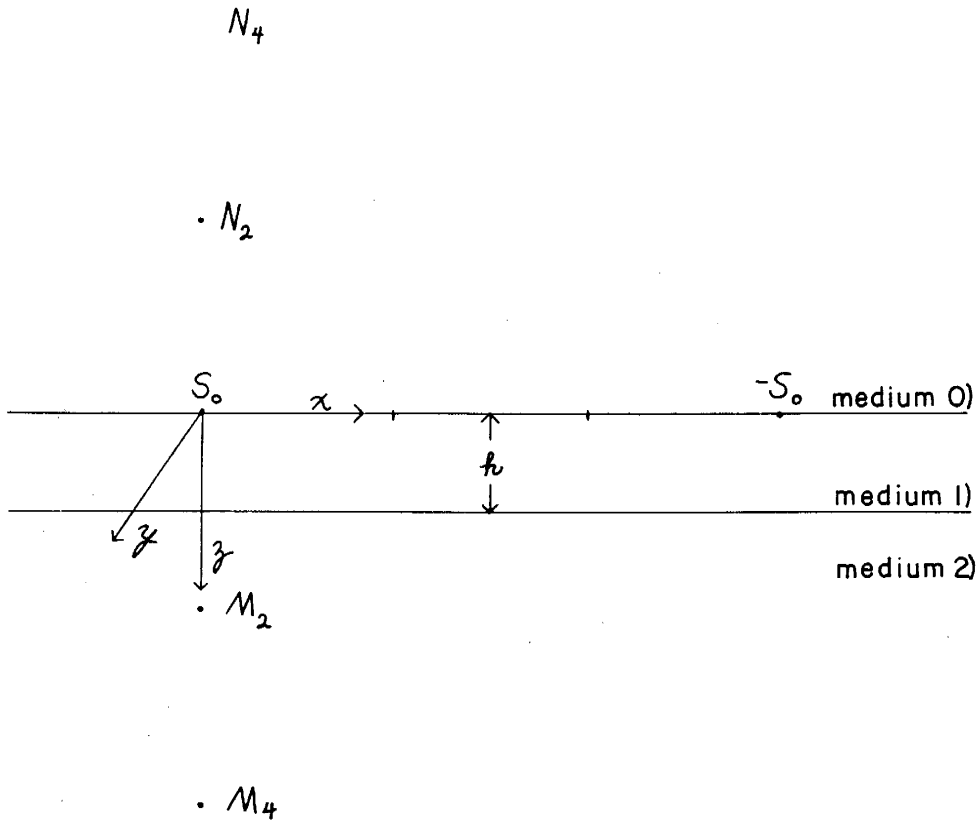

Figure 4

and medium 1), etc. Thus two infinite series of images N_{2k} and M_{2k} result. It is seen that N_{2k} and M_{2k} are at a distance of $2kh (k = 1, 2, 3 \ldots)$ from the origin at S_o.

Roman (1931) has shown that the potential Ψ_0 at any point inside medium 0) is given by

$$\Psi_0 = \frac{{}_0S_0}{\sqrt{x^2+y^2+z^2}} + \sum_{k=1}^{\infty} \frac{{}_0M_2k}{\sqrt{x^2+y^2+(2kh-z)^2}} \quad , \tag{13}$$

at a point in the overburden

$$\Psi_1 = \frac{{}_1S_0}{\sqrt{x^2+y^2+z^2}} + \sum_{k=1}^{\infty} \left(\frac{{}_1M_2k}{\sqrt{x^2+y^2+(2kh-z)^2}} + \frac{{}_1N_2k}{\sqrt{x^2+y^2+(2kh+z)^2}} \right) \quad , \tag{14}$$

and in the aquifer

$$\Psi_2 = \frac{{}_2S_0}{\sqrt{x^2+y^2+z^2}} + \sum_{k=1}^{\infty} \frac{{}_2N_2k}{\sqrt{x^2+y^2+(2kh+z)^2}} \quad . \tag{15}$$

The subscripts before the constants S, N, and M indicate the medium in which the potential is being described. The subscripts after the constants are indicative of the distance $2kh$ of the particular image from the origin. In order to get the expression for Ψ_2 in terms of more fundamental quantities, we must evaluate the source and image constants by substituting the above potential relations into the boundary conditions (1) and (2).

Solving for these constants and substituting them into equation (15) the expression for the potential in the aquifer becomes,

$$\Psi_2 = \frac{I\rho_1(Q_2+1)}{2\pi} \sum_{k=0}^{\infty} \frac{Q_2^k}{\sqrt{x^2+y^2+(2kh+z)^2}} \tag{16}$$

where $Q_2 = \frac{\rho_2-\rho_1}{\rho_2+\rho_1}$. Since there are two current electrodes in the Wenner configuration, the total potential in medium 2) results from the superposition of the potentials due to each

electrode. In the Wenner configuration the coordinates of the other current electrode are $(3a,0,0)$, and the distance between it and any point P is $\sqrt{(x-3a)^2+y^2+z^2}$. Thus the total potential Ψ_2 can be written as

$$\Psi_2 = \frac{I\rho_1(Q_2+1)}{2\pi}\sum_{k=0}^{\infty} Q_2^k\left(\frac{1}{\sqrt{x^2+y^2+(2kh+z)^2}} - \frac{1}{\sqrt{(x-3a)^2+y^2+(2kh+z)^2}}\right) . \quad (17)$$

From equations (7) and (8), the expression for the dipole moment is

$$\vec{P} = A_2 \nabla \Psi \quad , \quad (18)$$

where A_2 contains the polarization constants. Considering the components of $\vec{P}$ separately,

$$P_x = A_2 \frac{\partial \Psi_2}{\partial x} \quad , \quad (19a)$$

$$P_y = A_2 \frac{\partial \Psi_2}{\partial y} \quad , \quad (19b)$$

and

$$P_z = A_2 \frac{\partial \Psi_2}{\partial z} \quad . \quad (19c)$$

Differentiating equation (17) and substituting it into (19) yields

$$P_x = \frac{I A_2 \rho_1(Q_2+1)}{2\pi}\sum_{k=0}^{\infty} Q_2^k\left[\frac{x-3a}{\left[(x-3a)^2+y^2+(2kh+z)^2\right]^{3/2}} - \frac{x}{\left[x^2+y^2+(2kh+z)^2\right]^{3/2}}\right] , \quad (20a)$$

$$P_y = \frac{I A_2 \rho_1(Q_2+1)}{2\pi}\sum_{k=0}^{\infty} Q_2^k\left[\frac{y}{\left[(x-3a)^2+y^2+(2kh+z)^2\right]^{3/2}} - \frac{y}{\left[x^2+y^2+(2kh+z)^2\right]^{3/2}}\right] , \quad (20b)$$

and

$$P_y = \frac{I A_2 \rho_1 (Q_2+1)}{2\pi} \sum_{k=0}^{\infty} Q_2^k \left[\frac{2kh+z}{\left[(x-3a)^2+y^2+(2kh+z)^2\right]^{\frac{3}{2}}} - \frac{2kh+z}{\left[x^2+y^2+(2kh+z)^2\right]^{\frac{3}{2}}} \right] . \quad (20c)$$

The relation between $\Delta\phi$ and P is

$$\Delta\phi = \int_{\text{aquifer}} \frac{|\vec{P}|}{4\pi\varepsilon} \left(\frac{\cos\theta_3}{r_3^2} - \frac{\cos\theta_4}{r_4^2} \right) d\tau \, . \quad (21)$$

From Figure 2 it can be seen that

$$r_3 = \sqrt{(x-a)^2+y^2+z^2}$$

and (22)

$$r_4 = \sqrt{(x-2a)^2+y^2+z^2} \, ,$$

and that

$$\cos\theta_{x_1} = -\frac{x-a}{r_1} \, , \quad \cos\theta_{x_2} = -\frac{x-2a}{r_2} \, ,$$

$$\cos\theta_{y_1} = -\frac{y}{r_1} \, , \quad \cos\theta_{y_2} = -\frac{y}{r_2} \, , \quad (23)$$

$$\cos\theta_{z_1} = -\frac{z}{r_1} \, , \quad \cos\theta_{z_2} = -\frac{z}{r_2} \, .$$

Using equation (21), the difference in potential between the non-polarizing electrodes is

$$\Delta\phi_2 = \int_{\text{aquifer}} \frac{1}{4\pi\varepsilon} \left[P_x \left(\frac{\cos\theta_{x_3}}{r_3^2} - \frac{\cos\theta_{x_4}}{r_4^2} \right) \right.$$

$$\left. + P_y \left(\frac{\cos\theta_{y_3}}{r_3^2} - \frac{\cos\theta_{y_4}}{r_4^2} \right) + P_z \left(\frac{\cos\theta_{z_3}}{r_3^2} - \frac{\cos\theta_{z_4}}{r_4^2} \right) \right] d\tau \, . \quad (24)$$

The quantity ε is related to both ε_1 and ε_2. Its value will be discussed later.

and

$$P_y = \frac{I A_2 \rho_1 (Q_2+1)}{2\pi} \sum_{k=0}^{\infty} Q_2^k \left[\frac{2kh+z}{\left[(x-3a)^2+y^2+(2kh+z)^2\right]^{\frac{3}{2}}} - \frac{2kh+z}{\left[x^2+y^2+(2kh+z)^2\right]^{\frac{3}{2}}} \right]. \quad (20c)$$

The relation between $\Delta\phi$ and P is

$$\Delta\phi = \int_{\text{aquifer}} \frac{|\vec{P}|}{4\pi\varepsilon} \left(\frac{\cos\theta_3}{r_3^2} - \frac{\cos\theta_4}{r_4^2} \right) d\tau \, . \quad (21)$$

From Figure 2 it can be seen that

$$r_3 = \sqrt{(x-a)^2+y^2+z^2}$$

and (22)

$$r_4 = \sqrt{(x-2a)^2+y^2+z^2} \, ,$$

and that

$$\cos\theta_{x_1} = -\frac{x-a}{r_1} \, , \quad \cos\theta_{x_2} = -\frac{x-2a}{r_2} \, ,$$

$$\cos\theta_{y_1} = -\frac{y}{r_1} \, , \quad \cos\theta_{y_2} = -\frac{y}{r_2} \, , \quad (23)$$

$$\cos\theta_{z_1} = -\frac{z}{r_1} \, , \quad \cos\theta_{z_2} = -\frac{z}{r_2} \, .$$

Using equation (21), the difference in potential between the non-polarizing electrodes is

$$\Delta\phi_2 = \int_{\text{aquifer}} \frac{1}{4\pi\varepsilon} \left[P_x \left(\frac{\cos\theta_{x_3}}{r_3^2} - \frac{\cos\theta_{x_4}}{r_4^2} \right) \right.$$

$$\left. + P_y \left(\frac{\cos\theta_{y_3}}{r_3^2} - \frac{\cos\theta_{y_4}}{r_4^2} \right) + P_z \left(\frac{\cos\theta_{z_3}}{r_3^2} - \frac{\cos\theta_{z_4}}{r_4^2} \right) \right] d\tau \, . \quad (24)$$

The quantity ε is related to both ε_1 and ε_2. Its value will be discussed later.

Substituting equations (20), (22), and (23) into equation (24), we have an expression for the potential difference between the nonpolarizing electrodes due to a polarizable aquifer.

$$\Delta\phi_2=\frac{I A_2 \rho_1(Q_2+1)}{8\pi^2\varepsilon}\int_h\int_{-\infty}^{+\infty}\sum_{k=0}^{\infty}Q_2^k\left(\left(\frac{x-3a}{\left[(x-3a)^2+y^2+(2kh+z)^2\right]^{3/2}}-\frac{x}{\left[x^2+y^2+(2kh+z)^2\right]^{3/2}}\right)\right.$$
$$\left(\frac{x-2a}{\left[(x-2a)^2+y^2+z^2\right]^{3/2}}-\frac{x-a}{\left[(x-a)^2+y^2+z^2\right]^{3/2}}\right)+$$
$$\left(\frac{y}{\left[(x-3a)^2+y^2+(2kh+z)^2\right]^{3/2}}-\frac{y}{\left[x^2+y^2+(2kh+z)^2\right]^{3/2}}\right)$$
$$\left(\frac{y}{\left[(x-2a)^2+y^2+z^2\right]^{3/2}}-\frac{y}{\left[(x-a)^2+y^2+z^2\right]^{3/2}}\right)+ \qquad (25)$$
$$\left(\frac{2kh+z}{\left[(x-3a)^2+y^2+(2kh+z)^2\right]^{3/2}}-\frac{2kh+z}{\left[x^2+y^2+(2kh+z)^2\right]^{3/2}}\right)$$
$$\left.\left(\frac{z}{\left[(x-2a)^2+y^2+z^2\right]^{3/2}}-\frac{z}{\left[(x-a)^2+y^2+z^2\right]^{3/2}}\right)\right\}dx\,dy\,dz$$

or

$$\Delta\phi_2=\frac{I A_2 \rho_1(Q_2+1)}{8\pi^2\varepsilon}\iiint\sum_{k=0}^{\infty}Q_2^k\left[\frac{(x-3a)(x-2a)+y^2+(2kh+z)z}{\left\{\left[(x-3a)^2+y^2+(2kh+z)^2\right]\left[(x-2a)^2+y^2+z^2\right]\right\}^{3/2}}\right.$$
$$-\frac{(x-3a)(x-a)+y^2+(2kh+z)z}{\left\{\left[(x-3a)^2+y^2+(2kh+z)^2\right]\left[(x-a)^2+y^2+z^2\right]\right\}^{3/2}}$$
$$-\frac{x(x-2a)+y^2+(2kh+z)z}{\left\{\left[x^2+y^2+(2kh+z)^2\right]\left[(x-2a)^2+y^2+z^2\right]\right\}^{3/2}} \qquad (26)$$
$$\left.+\frac{x(x-a)+y^2+(2kh+z)z}{\left\{\left[x^2+y^2+(2kh+z)^2\right]\left[(x-a)^2+y^2+z^2\right]\right\}^{3/2}}\right]dx\,dy\,dz\ .$$

When $3a-x$ is substituted for x in the appropriate pair of the four integrals, which is justified since the interval of inte-

gration extends from $-\infty$ to $+\infty$, equation (26) simplifies to

$$\Delta\phi_2=\frac{I A_2 \rho_1 (Q_2+1)}{4\pi^2 \varepsilon}\int_{h=-\infty}^{+\infty}\int\int\sum_{k=0}^{\infty} Q_2^k\left\{\frac{x(x-a)+y^2+(2kh+z)z}{[x^2+y^2+(2kh+z)^2]^{3/2}}\right.$$
$$\left.-\frac{(x-3a)(x-a)+y^2+(2kh+z)z}{[(x-3a)^2+y^2+(2kh+z)^2]^{3/2}}\right\}\frac{dx\,dy\,dz}{[(x-a)^2+y^2+z^2]^{3/2}}\quad . \tag{27}$$

Since the expression is symmetrical with respect to the y coordinate,

$$\int_{-\infty}^{+\infty} f(y^2)\,dy = 2\int_{0}^{+\infty} f(y^2)\,dy \quad .$$

Thus

$$\Delta\phi_2=\frac{I A_2 \rho_1 (Q_2+1)}{2\pi^2 \varepsilon}\int_{h=0}^{+\infty}\int_{-\infty}^{+\infty}\int\sum_{k=0}^{\infty} Q_2^k\left(\frac{x(x-a)+y^2+(2kh+z)z}{[x^2+y^2+(2kh+z)^2]^{3/2}}\right.$$
$$\left.-\frac{(x-3a)(x-a)+y^2+(2kh+z)z}{[(x-3a)^2+y^2+(2kh+z)^2]^{3/2}}\right)\frac{dx\,dy\,dz}{[(x-a)^2+y^2+z^2]^{3/2}}\quad . \tag{28}$$

Coordinates of the integrand are transformed into units of a by letting $x=a\xi$, $y=a\sigma$, $z=a\delta$ and $h=aH$.

$$\Delta\phi_2=\frac{I A_2 \rho_1 (Q_2+1)}{2\pi^2 \varepsilon a}\int_{H=0}^{+\infty}\int_{-\infty}^{+\infty}\int\sum_{k=0}^{\infty} Q_2^k\left[\frac{\xi(\xi-1)+\sigma^2+(2kH+\delta)\delta}{[\xi^2+\sigma^2+(2kH+\delta)^2]^{3/2}}\right.$$
$$\left.-\frac{(\xi-3)(\xi-1)+\sigma^2+(2kH+\delta)\delta}{[(\xi-3)^2+\sigma^2+(2kH+\delta)^2]^{3/2}}\right]\frac{d\xi\,d\sigma\,d\delta}{[(\xi-1)^2+\sigma^2+\delta^2]^{3/2}}\quad . \tag{29}$$

Since

$$V=\frac{I\rho_a}{2\pi a}\quad , \tag{30}$$

$\frac{\Delta\Phi_2}{V}$ finally becomes,

$$\frac{\Delta\Phi_2}{V} = \frac{A_2(Q_2+1)\rho_1}{\pi\varepsilon\,\rho_a} \iiint_{H\,0-\infty}^{+\infty} \sum_{k=0}^{\infty} Q_2^k \left[\frac{\xi(\xi-1)+\sigma^2+(2kH+\delta)\delta}{[\xi^2+\sigma^2+(2kH+\delta)^2]^{3/2}} - \frac{(\xi-3)(\xi-1)+\sigma^2+(2kH+\delta)\delta}{[(\xi-3)^2+\sigma^2+(2kH+\delta)^2]^{3/2}} \right] \frac{d\xi\,d\sigma\,d\delta}{[(\xi-1)^2+\sigma^2+\delta^2]^{3/2}} \quad (31)$$

Interchanging summation and integration signs,

$$\frac{\Delta\Phi_2}{V} = \frac{A_2(Q_2+1)\rho_1}{\pi\varepsilon\,\rho_a} \sum_{k\,0}^{\infty} Q_2^k \iiint_{H\,0-\infty}^{+\infty} \left[\frac{\xi(\xi-1)+\sigma^2+(2kH+\delta)\delta}{[\xi^2+\sigma^2+(2kH+\delta)^2]^{3/2}} - \frac{(\xi-3)(\xi-1)+\sigma^2+(2kH+\delta)\delta}{[(\xi-3)^2+\sigma^2+(2kH+\delta)^2]^{3/2}} \right] \frac{d\xi\,d\sigma\,d\delta}{[(\xi-1)^2+\sigma^2+\delta^2]^{3/2}} \quad (32)$$

The integral portion of equation (32) was solved numerically on a digital computer at Los Alamos, New Mexico. A mesh system including 37 values of ξ, 23 values of σ and 19 values of δ (a total of 16,169 mesh points) spaced in the manner indicated in Table 1, gave values of the integral to within a maximum error of 10%.

The integral was evaluated for values of H = 0.1, 0.2, 0.4, 0.8, 1.6 and 3.2. For H = 0.1, as many as 12 terms of the series are required to maintain less than 10% error. As the values of H increase, the rate of convergence increases so that fewer terms are required. The rate of convergence decreases with increasing magnitude of Q_2. This may partially explain the lack of conformity of the Q_2 = -0.9 curve (Figure 6).

Values of $\frac{\rho_1}{\rho_a}$ for $Q_2 = \pm 0.3, \pm 0.6, \pm 0.9$ were obtained from Roman's tables (Roman, 1934). The values of $\frac{\rho_1}{\rho_a}$ at $\frac{a}{h} = 10$ had to be approximated so that at this point $\frac{\Delta\Phi_2}{V}$ may

TABLE 1

Mesh System

ξ	-1 3/8 (3/16) + 1/2;	1/2 (3/32) 1 5/8;	1 5/8 (3/16) 4 1/4
σ	0 (.1) 1;	1 (.2) 2.2;	2.2 (.4) 4.6
δ	.1 (.05) .4;	.4 (.1) .8;	.8 (.4) 4.0

TABLE 2

Computed Values of the Integral

Q_2 \ $\frac{a}{h}$	10	5	2.5	1.25	0.625	0.3125
	0.1	0.2	0.4	0.8	1.6	3.2
-0.9	0.8149	0.8017	0.6892	0.3432	0.0753	0.0052
-0.6	0.9714	0.9233	0.7582	0.3603	0.0774	0.0052
-0.3	1.1776	1.0938	0.8439	0.3805	0.0793	0.0054
0.0	1.4944	1.3326	0.9517	0.4041	0.0820	0.0054
+0.3	2.0304	1.6888	1.0926	0.4325	0.0847	0.0054
+0.6	3.1039	2.2777	1.2888	0.4677	0.0883	0.0056
+0.9	6.0362	3.4363	1.5930	0.5163	0.0929	0.0057

TABLE 3

Computed Values of Equation (33)

Q_2 \ $\frac{a}{h}$	10	5	2.5	1.25	0.625	0.3125
-0.9	1.61	1.2918	0.3776	0.0591	0.0084	0.0005
-0.6	1.54	1.3513	0.7617	0.2043	0.0334	0.0021
-0.3	1.53	1.3455	0.8894	0.3159	0.0577	0.0038
0.0	1.4944	1.3326	0.9517	0.4041	0.0820	0.0054
+0.3	1.48	1.3160	0.9875	0.4761	0.1057	0.0070
+0.6	1.44	1.2955	1.0091	0.5578	0.1296	0.0088
+0.9	1.43	1.2495	1.0157	0.586	0.1540	0.0106

exceed the 10% maximum error.

Table 2 contains the computed values of the integral of equation (32). Table 3 contains the computed values of

$$\frac{\pi\varepsilon}{A_2}\frac{\Delta\phi_2}{V}=(Q_2+1)\frac{\rho_1}{\rho_2}\sum_{k=0}^{\infty}Q_2^k\iiint_{H\,0\,-\infty}^{+\infty}\left[\frac{\xi(\xi-1)+\sigma^2+(2kH+\delta)\delta}{[\xi^2+\sigma^2+(2kH+\delta)^2]^{3/2}}\right.$$
$$\left.-\frac{(\xi-3)(\xi-1)+\sigma^2+(2kH+\delta)\delta}{[(\xi-3)^2+\sigma^2+(2kH+\delta)^2]^{3/2}}\right]\frac{d\xi\,d\sigma\,d\delta}{[(\xi-1)^2+\sigma^2+\delta^2]^{3/2}}\quad . \qquad (33)$$

Figures 5 and 6 are a plot of the values taken from Table 3 where $\frac{a}{h}$ is plotted on the abscissa. Because $\frac{\Delta\phi_2}{V}$ differs from the values of the ordinate only by the constant factor $\frac{A_2}{\pi\varepsilon}$, it exhibits the same dependence on $\frac{a}{h}$.

One of the more striking disclosures apparent from these curves is the small influence the resistivity contrast has on the magnitude of $\frac{\Delta\phi_2}{V}$. At the value $\frac{a}{h}=5$, $\frac{\Delta\phi_2}{V}$ for all resistivity contrasts is practically the same. Also, at this point $\frac{\Delta\phi_2}{V}$ has nearly reached its full magnitude.

Paul Kintzinger (1956) made measurements on a model in a tank which approximately satisfied the conditions of the earth model for which Figures 5 and 6 were computed, namely, a non-polarizing upper layer and a polarizable, infinitely deep lower layer. Figure 7 is a plot of the theoretical values of $Q_2 = -0.6$ and 0.0 taken from Figure 6 with the experimental results (dashed) for the same Q_2 values superimposed upon them. The scale of the ordinates of the experimental curves was adjusted to fit the theoretical curves. The fact that the experimental curves lie above the theoretical ones for the smaller

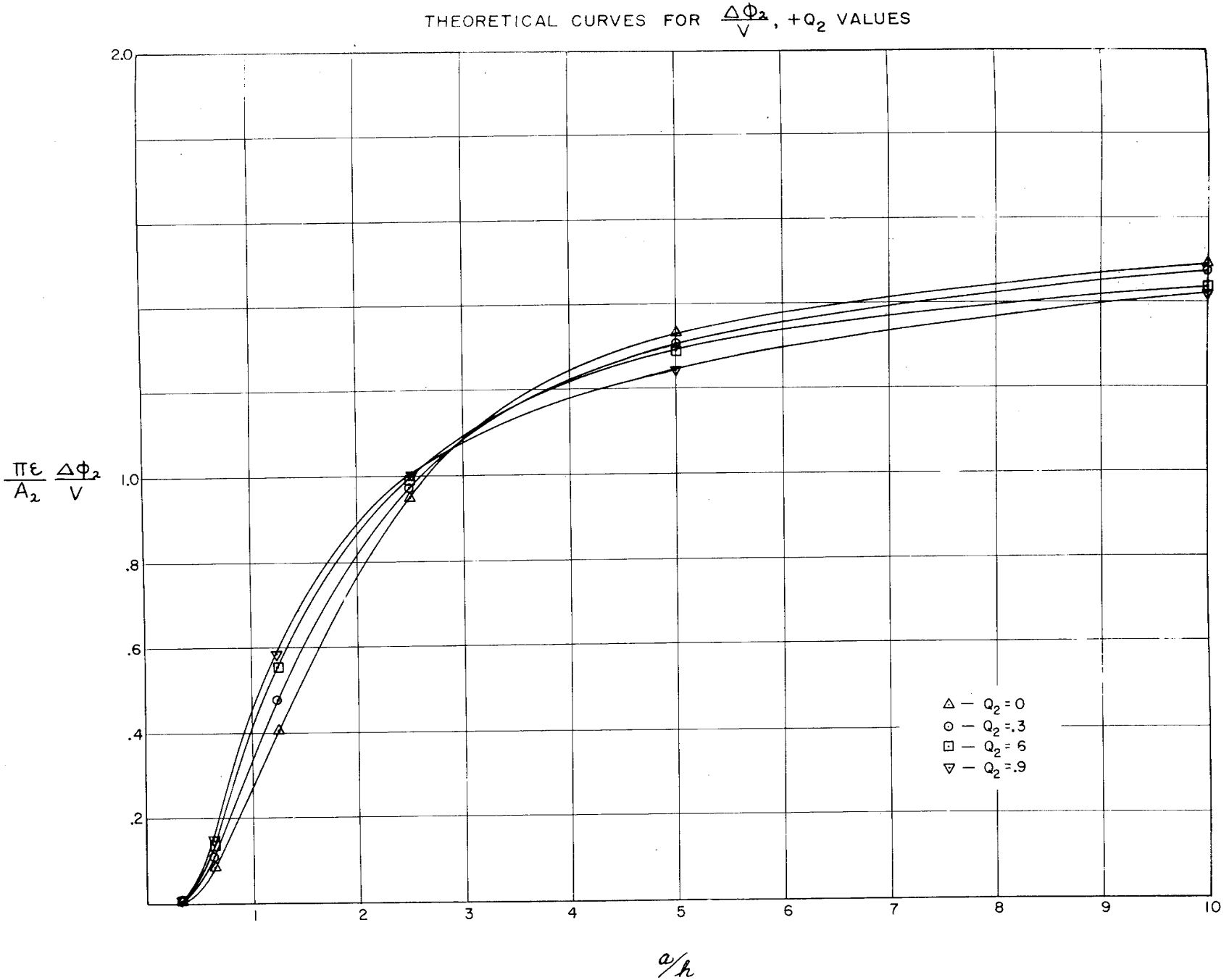
THEORETICAL CURVES FOR $\frac{\Delta\Phi_2}{V}$, $+Q_2$ VALUES
$\frac{\pi\epsilon}{A_2}\frac{\Delta\Phi_2}{V}$
2.0
1.0
.8
.6
.4
.2
1
2
3
4
5
6
7
8
9
10
a/h
△ — Q_2 = 0
⊙ — Q_2 = .3
⊡ — Q_2 = .6
▽ — Q_2 = .9

Figure 5

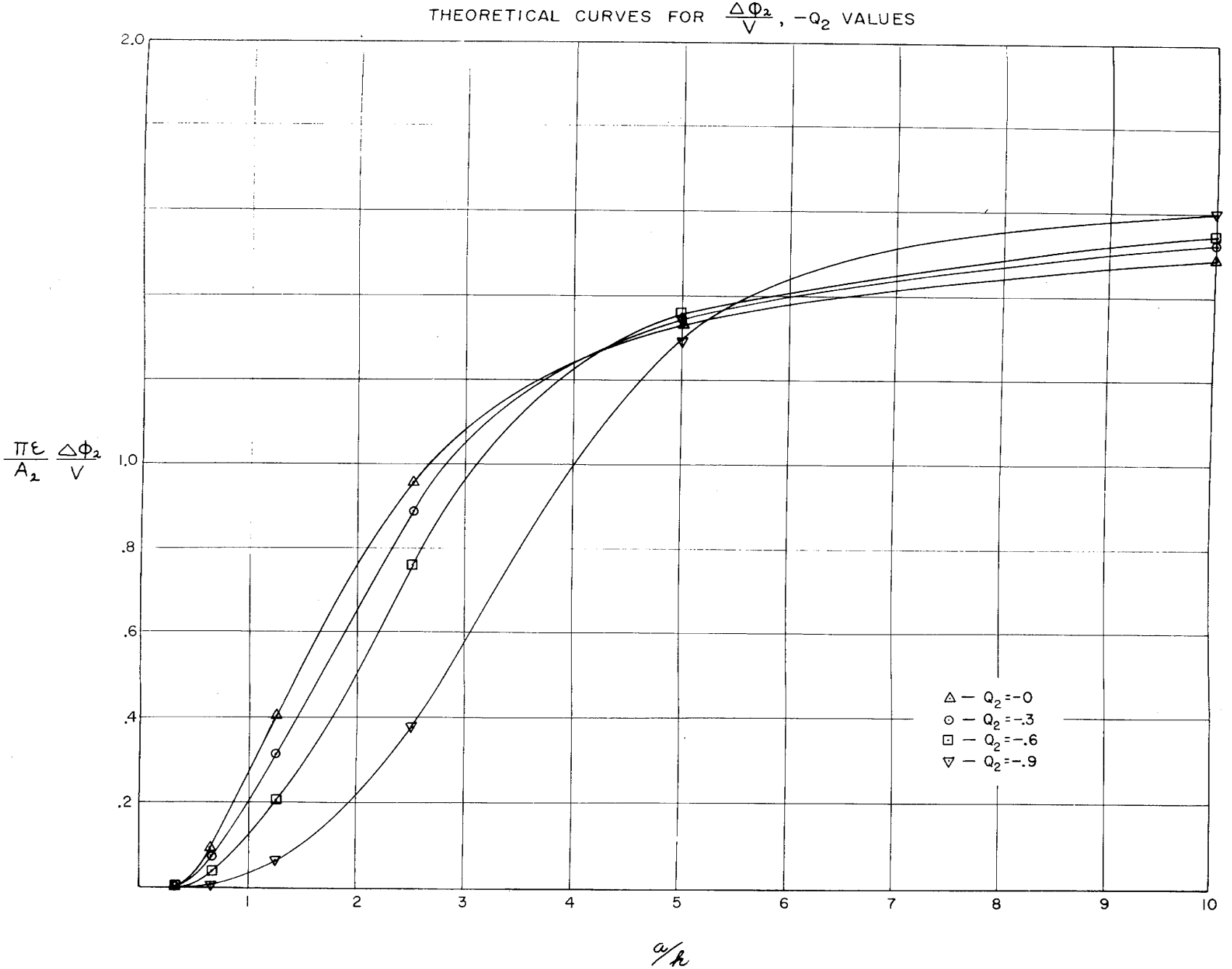
THEORETICAL CURVES FOR $\frac{\Delta\Phi_2}{V}$, $-Q_2$ VALUES
$\frac{\pi\epsilon}{A_2}\frac{\Delta\Phi_2}{V}$
2.0
1.0
.8
.6
.4
.2
1
2
3
4
5
6
7
8
9
10
a/h
△ — Q_2 = -0
⊙ — Q_2 = -.3
⊡ — Q_2 = -.6
▽ — Q_2 = -.9

Figure 6

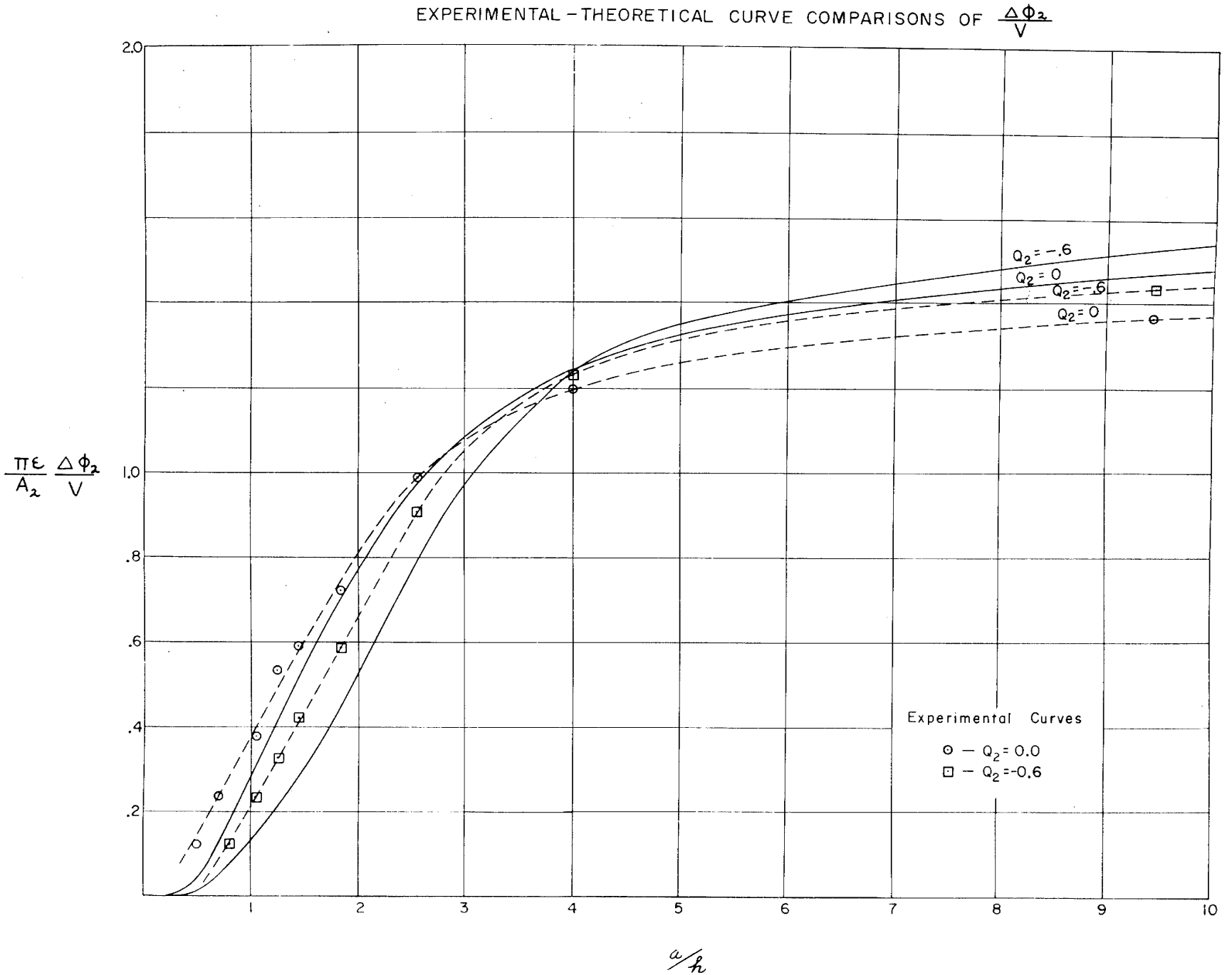
EXPERIMENTAL – THEORETICAL CURVE COMPARISONS OF $\frac{\Delta\phi_2}{V}$
$\frac{\pi\epsilon}{A_2}\frac{\Delta\phi_2}{V}$
2.0
1.0
.8
.6
.4
.2
1
2
3
4
5
6
7
8
9
10
$Q_2 = -.6$
$Q_2 = 0$
$Q_2 = -.6$
$Q_2 = 0$
Experimental Curves
⊙ — $Q_2 = 0.0$
⊡ — $Q_2 = -0.6$
a/h

Figure 7

values of $\frac{a}{h}$ is explained by the partial leaching of salts from the polarizable medium by the overlying water which Kintzinger (1956) used as the non-polarizable overburden.

The fair agreement between theoretical and experimental points gives support to the validity of the assumptions made for the calculations. In particular, it seems justifiable to treat the aquifer as a dielectric medium.

In the derivation of the induced polarization ratio $\frac{\Delta\Phi_2}{V}$ due to the lower medium, the current distribution is attributed to the resistivities of both media. The presence of polarizability does not affect the current distribution. It is therefore evident that an expression for $\frac{\Delta\Phi_1}{V}$ for a polarizable upper layer, could be added to $\frac{\Delta\Phi_2}{V}$ for the lower layer to give the total induced-polarization effect. Starting with equation (14) the expression for $\frac{\Delta\Phi_1}{V}$ is derived in a manner similar to that for $\frac{\Delta\Phi_2}{V}$.

$$\Delta\phi_1 = \frac{I A_1 \rho_1}{8\pi^2 \varepsilon_1} \iiint_{k=-\infty}^{+\infty} \left\{ \frac{(x-3a)(x-2a)+y^2+z^2}{\{[(x-3a)^2+y^2+z^2][(x-2a)^2+y^2+z^2]\}^{3/2}} \right.$$

$$- \frac{x(x-2a)+y^2+z^2}{[x^2+y^2+z^2][(x-2a)^2+y^2+z^2]\}^{3/2}} - \frac{(x-3a)(x-a)+y^2+z^2}{[(x-3a)^2+y^2+z^2][(x-a)^2+y^2+z^2]\}^{3/2}}$$

$$+ \frac{x(x-a)+y^2+z^2}{\{[x^2+y^2+z^2][(x-a)^2+y^2+z^2]\}^{3/2}} + \sum_{k=1}^{\infty} Q_2^k \left[\frac{x(x-a)+y^2+(2kh-z)z}{\{[x^2+y^2+(2kh-z)^2][(x-a)^2+y^2+z^2]\}^{3/2}} \right.$$

$$- \frac{x(x-2a)+y^2+(2kh-z)z}{\{[x^2+y^2+(2kh-z)^2][(x-2a)^2+y^2+z^2]\}^{3/2}}$$

$$- \frac{(x-3a)(x-a)+y^2+(2kh-z)z}{\{[(x-3a)^2+y^2+(2kh-z)^2][(x-a)^2+y^2+z^2]\}^{3/2}} \qquad (34)$$

$$+ \frac{(x-3a)(x-2a)+y^2+(2kh-z)z}{\{[(x-3a)^2+y^2+(2kh-z)^2][(x-2a)^2+y^2+z^2]\}^{3/2}}$$

$$+ \frac{x(x-a)+y^2+(2kh+z)z}{\{[x^2+y^2+(2kh+z)^2][(x-a)^2+y^2+z^2]\}^{3/2}}$$

$$- \frac{x(x-2a)+y^2+(2kh+z)z}{\{[x^2+y^2+(2kh+z)^2][(x-2a)^2+y^2+z^2]\}^{3/2}}$$

$$- \frac{(x-3a)(x-a)+y^2+(2kh+z)z}{\{[(x-3a)^2+y^2+(2kh+z)^2][(x-a)^2+y^2+z^2]\}^{3/2}}$$

$$\left. \left. - \frac{(x-3a)(x-2a)+y^2+(2kh+z)z}{\{[(x-3a)^2+y^2+(2kh+z)^2][(x-2a)^2+y^2+z^2]\}^{3/2}} \right] \right\} dx\,dy\,dz \quad .$$

It should be noted that this equation is the same as (26) with the addition of the integrals containing $(2kh-z)$. At the present time these integrals have not been evaluated. However, the general form for the solution of the integral was experimentally determined by Paul Kintzinger (1956) for a Q_2 value of approximately + 0.6 (curve 1, Figure 9). Because of the similarity of the $\Delta\phi$ expressions it is believed that $\frac{\Delta\phi_1}{V}$ will have about the same resistivity dependence as $\frac{\Delta\phi_2}{V}$. Thus we can use Kintzinger's curve in conjunction with the $\frac{\Delta\phi_2}{V}$ curves developed in this paper to approximate field curves of different resistivity contrasts.

Consider the logarithmic plot of the field curve in Figure 8. The curve approaches the value 75 and 350 millivolt seconds/volt asymptotically. The ratio $350/75 = 4.67$ is the ratio of the polarization constants $\frac{A_2/\varepsilon_2}{A_1/\varepsilon_1}$. Thus in Figure 9 the curve for the upper layer 1) is plotted letting the relative maximum value be one at $\frac{a}{h}=0$. The value of the lower layer curve 2) at $\frac{a}{h}=10$ will be the asymptotic value of the field curve (4.67) minus the value of the upper layer curve at $\frac{a}{h}=10$. In this case it is $4.67 - 0.28 = 4.39$. This gives the scaling factor necessary to draw the lower layer curve 2). The field curve (dashed) is drawn so that it makes the best possible fit with curves 1)+2). The upper abscissa on the graph goes with the field curve. A comparison of the two abscissas shows that $\frac{a}{h}=1$ occurs at approximately 85 feet. This then is the predicted depth to water. In a nearby well the depth to water is 60 feet.

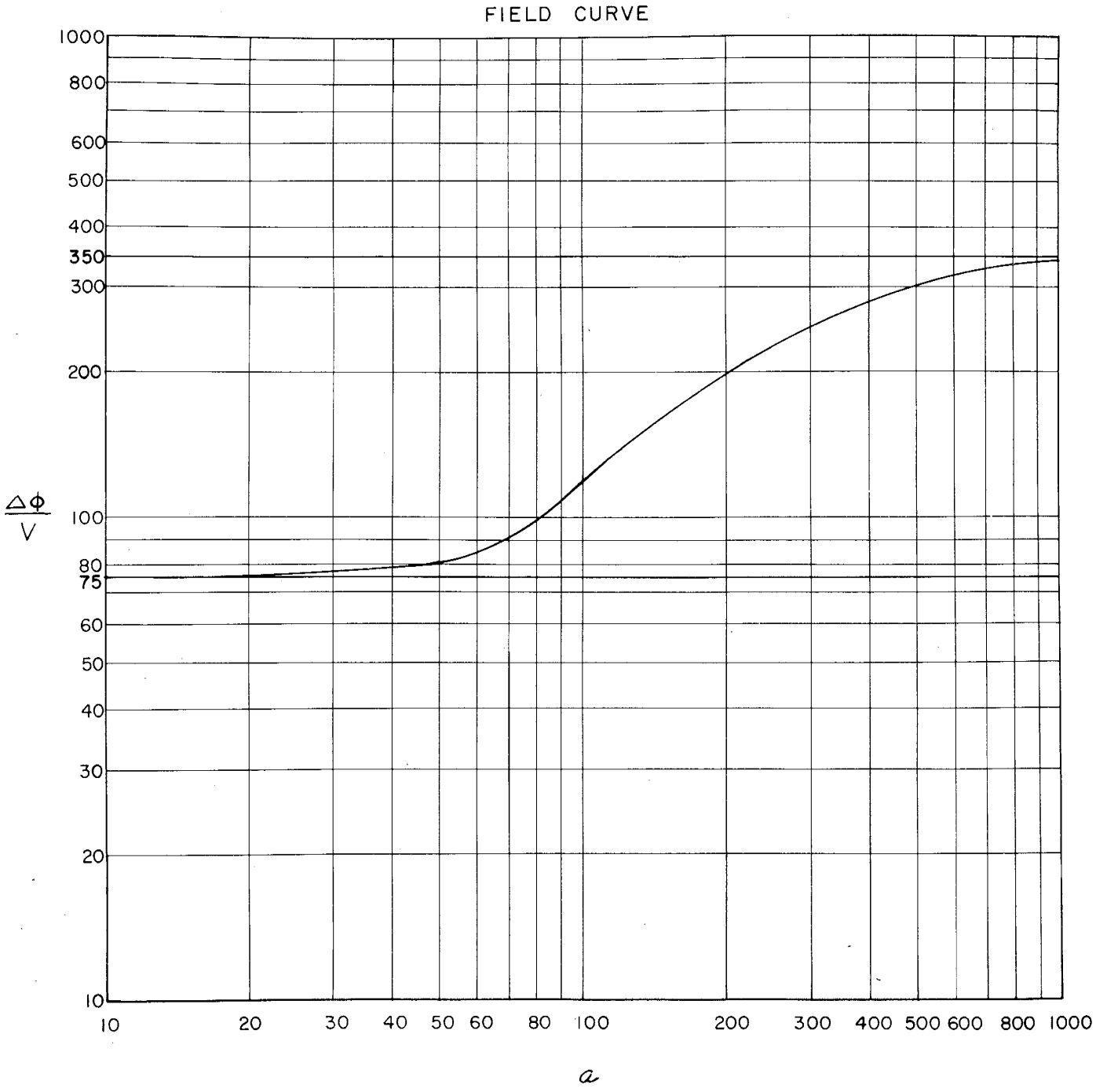
FIELD CURVE
1000
800
600
500
400
350
300
200
100
80
75
60
50
40
30
20
10
ΔΦ/V
10
20
30
40
50
60
80
100
200
300
400
500
600
800
1000
a

Figure 8

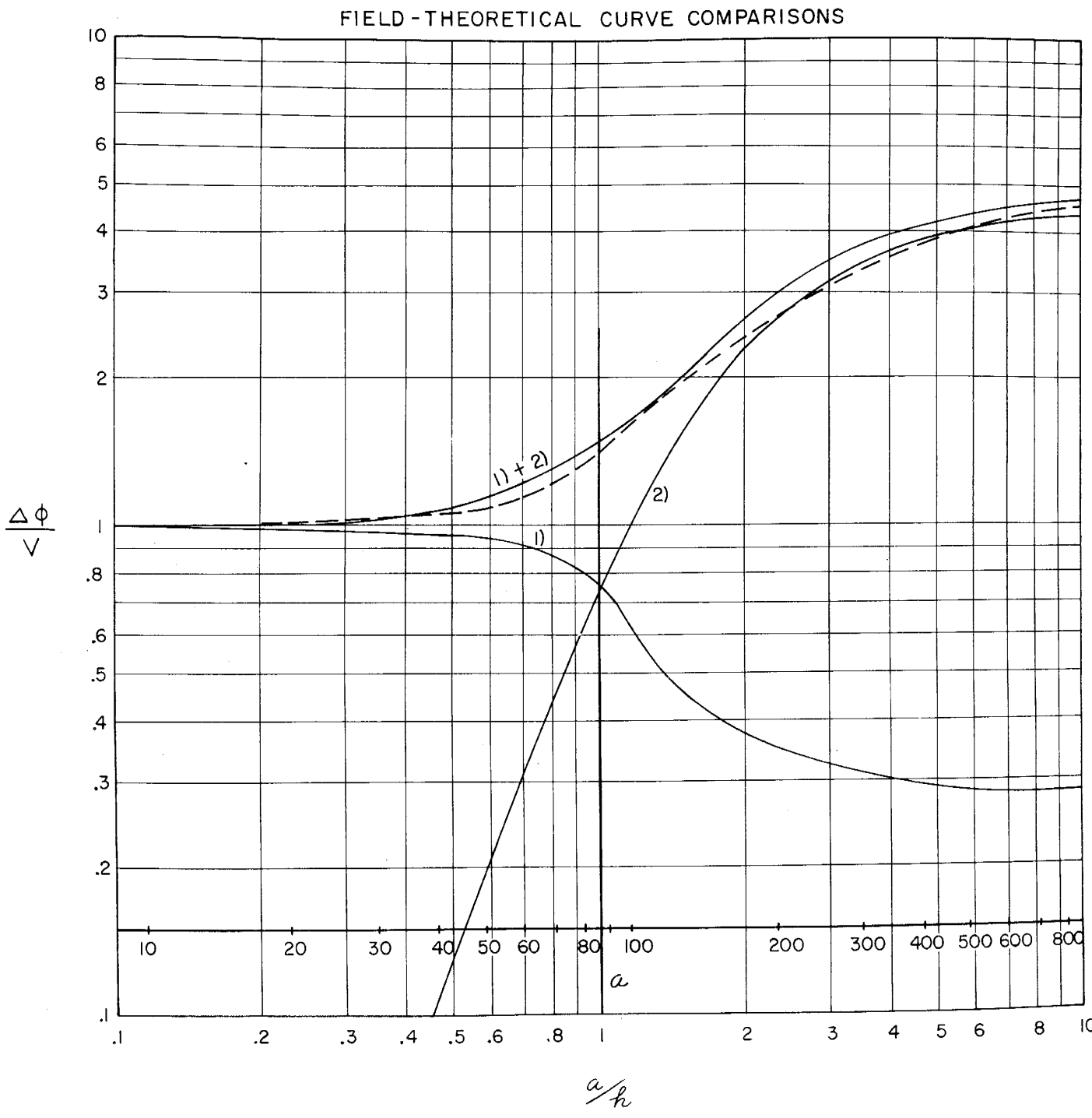
FIELD - THEORETICAL CURVE COMPARISONS
10
8
6
5
4
3
2
1
.8
.6
.5
.4
.3
.2
.1
Δφ/V
1) + 2)
2)
1)
10
20
30
40
50
60
80
100
200
300
400
500
600
800
a
.1
.2
.3
.4
.5
.6
.8
1
2
3
4
5
6
8
10
a/h

Figure 9

The principal cause of error is probably the lack of correspondence between the initial simplifying assumptions and the actual stratigraphic relations. In most cases there will be several resistivity and polarization horizons which will commonly be interfaces between non-uniform media. The interface itself will not be a surface of sharp contrast, but a zone of rapid change.

"DIELECTRIC CONSTANT" OF EARTH MATERIAL

A numerical value for the quazi-dielectric constant used in this calculation can be computed from field and laboratory measurements on wet earth materials. The maximum value calculated for the normalized instantaneous-decay potential, (see Figures 6 and 7) is approximately,

$$\frac{\Delta\Phi_2}{V} = \frac{A_2}{\pi\mathcal{E}_2}\,1.6 \quad . \tag{35}$$

For an electrode separation a, large compared to h, $\mathcal{E}$ is practically equal to $\mathcal{E}_2$. The dielectric constant K_e is defined as

$$K_e \equiv (1 + \chi_e) \tag{36}$$

and

$$\mathcal{E}_2 = \mathcal{E}_0(1 + \chi_{e_2}) \quad . \tag{36'}$$

It follows that

$$\frac{\Delta\Phi_2}{V} = \frac{1}{\pi}\left(1 - \frac{1}{K_{e_2}}\right)1.6 \quad . \tag{37}$$

Solving (37) for K_{e_2},

$$K_{e_2} = \frac{1.6}{1.6 - \pi\frac{\Delta\Phi}{V}} \quad . \tag{38}$$

The maximum values obtained for $\frac{\Delta\Phi}{V}$ from field data are approximately 10 millivolts per volt. Substituting this into (38),

K_e = 1.02. Since K_e is rather close to unity, $\mathcal{E}_2 \cong \mathcal{E}_o$. Thus, $\mathcal{E}$ in equation (24) and subsequent equations is also approximately equal to $\mathcal{E}_o$. This result seems incompatible with the low-frequency values for the dielectric constant of 10^6 found by G.V. Keller and P.H. Lecastro (1955) and 10^8 found by H.M. Evjen (1948).

This difference of a factor of 10^6 is interpreted as a divergence of two views on the definition of dielectric constant in moist earth materials. In this study the mathematical treatment was carried out by the equations of electrostatics for the sake of convenience. This treatment is valid only as long as one does not try to interpret the shape of the voltage-relaxation curve. This curve is not exponential but is hyperbolic (Kintzinger, 1956) and characteristic of ion-diffusion phenomena of electrochemistry. The dielectric constant is a measure of the displacement of bound charge in an electric field; it is not related to concentration and diffusion potentials. For example a condenser and a storage battery store electrical energy, but we do not ascribe the energy in the battery to the dielectric polarization of the electrolyte. The modest value of 1.02 for the dielectric constant obtained in this analysis is not necessarily related to any actual displacement of bound charges in the aquifer. It simply means that the induced electrochemical concentration and diffusion potentials are small compared to the potentials due to the energizing current.

CONCLUSION

A theoretical solution has been given for the two-layered induced-electrical-polarization problem for the case of a non-polarizable upper layer and a polarizable, infinitely deep lower layer. This solution has been shown to be in good agreement with data from a laboratory model and with a selected field curve.

It is believed that an attempt at a mathematical solution of a problem involving more than two layers would reach impractical proportions at the machine-computation stage. More complex distributions than the one treated in this paper are best studied on laboratory models.

BIBLIOGRAPHY

Evjen, H.M. (1948), Theory and Practice of Low-Frequency Electromagnetic Exploration: Geophysics, Vol. 13, pp. 584-594.

Keller, G.V. and Lecastro, P.H. (1955), Measurements of Electrical Resistivity and Dielectric Constants on Some Sandstone and Siltstone Cores: a paper presented at the 25th Annual Meeting of the Society of Exploration Geophysics.

Kintzinger, Paul R. (1956), A Laboratory Study of Induced Polarization: Ph.D. dissertation, New Mexico Institute of Mining and Technology.

Roman, Irwin (1931), How to Compute Tables for Determining Electrical Resistivity of Underlying Beds and Their Application to Geophysical Problems: U.S. Department of Commerce, Bureau of Mines, Technical Paper 502.

_____(1934), Some Interpretations of Earth-resistivity Data: AIME, Vol. 110, pp. 188, 189.